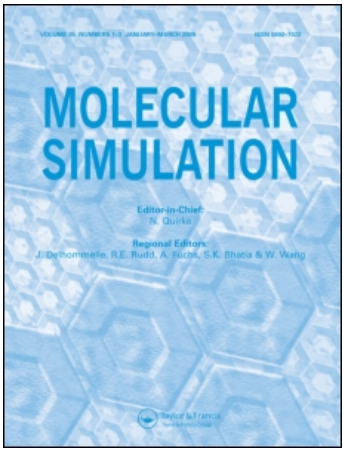

Molecular Simulation
Publication details, including instructions for authors and subscription information:
http://www.informaworld.com/smpp/title~content=t713644482

Structure-property relations between silicon-containing polyimides and their carbon-containing counterparts

Silke Pelzer[a]; Dieter Hofmann[a]
[a] Institute of Polymer Research, GKSS Research Center Geesthacht GmbH, Center for Biomaterial Development, Teltow, Germany

To cite this Article Pelzer, Silke and Hofmann, Dieter(2008) 'Structure-property relations between silicon-containing polyimides and their carbon-containing counterparts', Molecular Simulation, 34: 10, 1275 — 1282
To link to this Article: DOI: 10.1080/08927020802301888
URL: http://dx.doi.org/10.1080/08927020802301888

Molecular Simulation
Vol. 34, Nos. 10–15, September–December 2008, 1275–1282

Taylor & Francis
Taylor & Francis Group

Structure–property relations between silicon-containing polyimides and their carbon-containing counterparts

Silke Pelzer and Dieter Hofmann*

Institute of Polymer Research, GKSS Research Center Geesthacht GmbH, Center for Biomaterial Development, Teltow, Germany

(*Received 23 January 2008; final version received 24 June 2008*)

The present paper examines silicon (Si)-containing polyimides and their structural carbon (C)-containing counterparts regarding the relation between their oxygen permeability on the one hand and their microscopic structure on the other hand. There are significant differences in the fractional free volume and the mean squared displacement of Si-containing polyimides and their carbon counterparts. Compared to the C-polyimides the Si-ones have a greater free volume and show more mobility in the side-groups while the C-ones have a higher mobility in the backbone. These differences are typically connected with higher oxygen permeabilities in the respective Si-containing polymers.

Keywords: polyimides; silicon; fractional free volume; mean squared displacement; oxygen permeability

1. Introduction

Polyimides have been important membrane materials for gas separation for many years. Nevertheless there is still a strong need for further improved transport properties of these polymers, particularly regarding small molecule permeabilities and the selectivities for certain gas pairs. One problem is that improving the permeability normally goes along with a loss of selectivity. Numerous experiments have been performed to find out which factors might improve the permeability of a polyimide. Higher permeabilities can be reached by increasing the *ortho*-alkylation in the diamine, inserting $-CF^3$ groups, $SiO(Me)^2$, $Si(Me)^3$ or $C(Me)^3$ groups into the dianhydride, increasing rigidity and decreasing the diamine length or inserting bulky groups. It also turns out that producing a higher free volume leads to a higher permability [1–18]. Kim and coworkers [19–23] designed and examined various bulky Si-containing structures and their C-containing counterparts (Figure 1) with regard to their oxygen permeabilities (Table 1). The permeabilities between each pair of polyimide (e.g. Si-containing structure and C-containing counterpart) are, except for one case, higher for the Si than for the respective C-case. Concerning the diffusion (D) and the solubility (S), no experimental data for these types of polyimides are available. To validate the chosen models, experimental wide angle X-ray diffraction (WAXD) measurements reported in the literature [21] are available for two polyimides (A-1 and B-1). The major model properties considered to assess the critical structural differences between the polymers are the fractional free volume distribution (FFV) and the mean squared displacement (MSD) of the respective polymer atoms. These properties should be closely related to the transport properties of interest.

2. Computational details

The amorphous packing model construction and the atomistic simulations of the shown polymers have been investigated using the Accelrys Materials Studio® (MS) Modeling 3.2 program package and the COMPASS force field [24,25] followed by extensive equilibration procedures. Initial bulk polymer packing cells were created using the amorphous cell module of MS. The polymer chains were grown at 308 K under cubic periodic boundary conditions. To avoid packing algorithm related catenations and spearings of aromatic units, the initial packing density was very low (0.1 kg/m^3). As no experimental densities were provided through the literature, the Synthia tool of MS was used to estimate the densities of the different polyimides which were used to help creating the final basic cell for the systems (Table 2).

The atomistic chain segment packing cells employed in this work consist of about 4000–5000 atoms. For each of the polyimides, 10 independent packing models were obtained to increase the statistical significance of the results. The resulting initial packing models were equilibrated using force field parameter scaling [26] according to the procedure outlined in Table 3. The individual stages lasted for 1000 fs with a time step of 0.2 fs and were always preceded by a short energy minimisation of several 100 iterations.

After equilibrating the systems, the MSD results were obtained using the according routines of MS Modeling. For calculating the FFV the procedure described by Hofmann

*Corresponding author. Email: dieter.hofmann@gkss.de

ISSN 0892-7022 print/ISSN 1029-0435 online

DOI: 10.1080/08927020802301888
http://www.informaworld.com

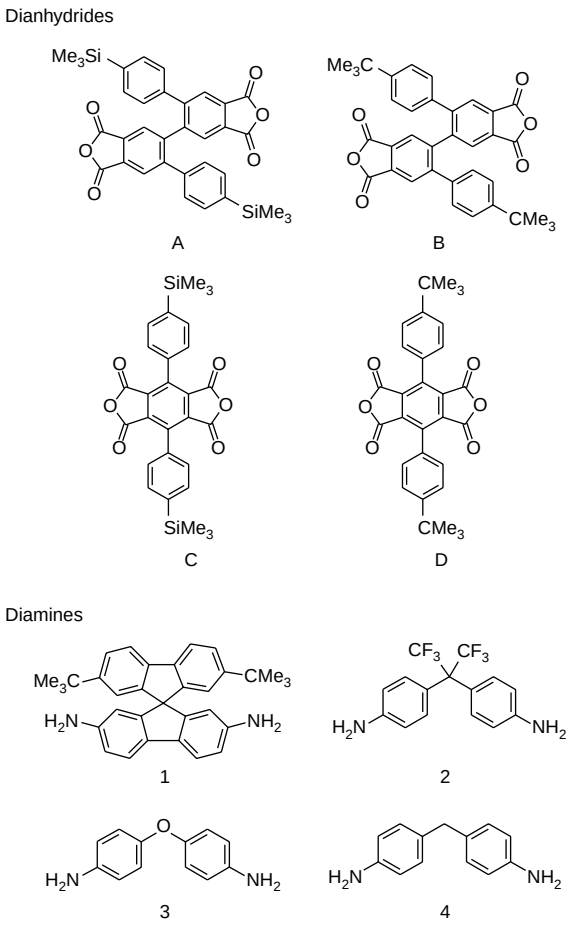

Figure 1. Dianhydride and diamine structures of the examined polyimides.

et al. [27] has been used. The van der Waals radii of the examined atoms were C: 1.55×10^{-10} m, H: 1.10×10^{-10} m, O: 1.73×10^{-10} m, F: 1.30×10^{-10} m and Si: 2.20×10^{-10} m. To determine the FFV and the fractional accessible volume (FAV) distributions, the overlaid three-dimensional probe molecule insertion grid had a grid-size δ of 0.5. An oxygen molecule (Ø: 1.73×10^{-10} m), a positronium (Ø: 1.1×10^{-10} m) and a particle with a diameter of 0.4×10^{-10} m were used as probe molecules. X-ray scattering calculations have been performed utilising the scattering routine implemented in the forcite module of MS Modeling. The used cutoff was 30×10^{-10} m to avoid artefacts, a model size correction of a 1.7×10^{-10} m radius was applied and the scattering intensity was plotted against the 2θ angle. Systematic conformational search procedures applying the discover module of the MS Modeling software of Accelrys were also performed to determine the energetic potential for the rotation around the central C—C-bond of some of the system.

Table 1. Experimental oxygen permeabilities of the chosen polyimides [19–23]; exp. setup: membrane thickness = 30–60 μm, T = RT, p_{feed} = 0.94 MPa.

Polyimide	P (O_2) [7,5005 × 10^{-18} m^2/s Pa]
A-1	121
A-2	105
A-3	61
A-4	52
B-1	52
B-2	110
B-3	43
B-4	31
C-2	56
C-3	32
C-4	14
D-2	50
D-3	20
D-4	13

Table 2. Simulation data.

Polymer	No. of repeat units	No. of atoms	Density (Synthia) [kg/m^3]	Average size of the periodic cell (10^{-10} m)
A1	37	4997	1.143	37.97
A2	45	4547	1.237	37.71
A3	45	4277	1.139	36.68
A4	45	4187	1.154	36.56
B1	37	4997	1.169	37.35
B2	45	4547	1.276	37.90
B3	45	4277	1.175	35.79
B4	45	4187	1.191	35.66
C2	45	4097	1.234	36.65
C3	55	4677	1.126	38.00
C4	55	4567	1.142	37.86
D2	45	4097	1.198	36.51
D3	55	4677	1.164	36.98
D4	55	4567	1.181	36.84

Table 3. Scaling factors of the five-step equilibration used for packing models.

Stage of equilibration	Scaling factor for the torsion term	Scaling factor for nonbonded interactions
1	10^{-3}	10^{-3}
2	10^{-2}	10^{-2}
3	1	10^{-3}
4	1	10^{-2}
5	1	1

3. Results and discussion

Experimental data is available from the literature for the oxygen and nitrogen permeabilities and for the polyimides A-1 and B-1 and WAXD measurements. For checking the quality of the models, calculations have been performed for A-1 and B-1 and WAXD as shown in Figure 2.

As can be seen, the calculated and the measured graphs are in good agreement with each other and therefore the chosen equilibration procedure, giving useful results for

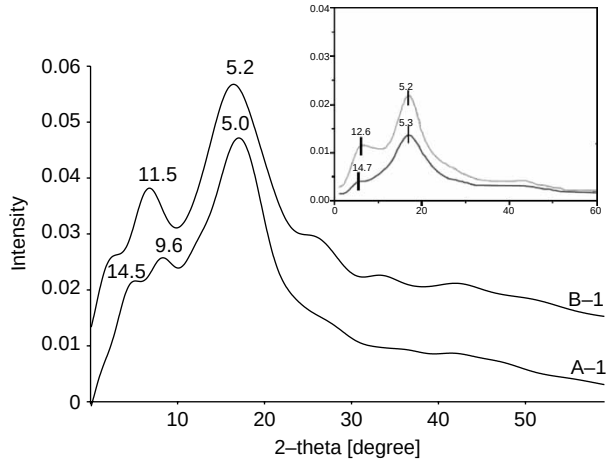

Figure 2. Comparison of the calculated (big graph) and the measured (small graph) [21] WAXD of A-1 and B-1. The given numbers in the graph show the calculated *d*-spacings in 10 nm scale. The additional peak at 9.6×10 nm is probably due to limited size effects and a slightly higher order in the model than the real system.

these polyimides, will be applied to all other polyimides as well. For further validation of the models, experimental information about the density ρ, the solubility coefficient S and the diffusion coefficient D would be helpful, as these values can also be calculated from the models. They are, however, not available in the literature. Concerning the permeability (P), experience shows that the comparing calculated and measured P-values is normally not sufficient. Computationally, the permeability will be calculated as the product of S and D and the deviations of the values of S and D compared to the experimental ones, via error propagation will lead to usually quite unsatisfying results of P. The direct model validation is therefore based on the already mentioned WAXD data for A-1 and B-1 indicating reasonably well-equilibrated models in these cases. Unfortunately these are the only WAXD data being measured experimentally, but since for more or less related other polyimides the same basic approach of model construction and equilibration was taken as for A-1 and B-1, it is assumed that also the other models are suited for evaluation. This view is further confirmed by the following approach where *in lieu* of experimental density data respective prediction from the Synthia module of MS were taken for comparison with the density values reached in the 1 Bar (NpT) MS-simulation, in Table 4.

Synthia is a method developed by Bicerano [2] and relates the properties of the polymer to a combination of four indices considering the composition and topology of the respective polymer repeat. Table 4 shows the Synthia results are in good agreement with the MD simulated results.

The main focus of this paper is the interpretation of the calculated free volume distribution and MSDs.

Table 4. Calculated density values given in kg/m^3.

Polymer	Synthia	NpT (average over 8–10 packing models)
A1	1.1434	1.1370
A2	1.2374	1.2375
A3	1.1398	1.1395
A4	1.1541	1.1512
B1	1.1691	1.1570
B2	1.2760	1.2746
B3	1.1747	1.1709
B4	1.1905	1.1902
C2	1.2340	1.2345
C3	1.1264	1.1250
C4	1.1420	1.1405
D2	1.2762	1.2985
D3	1.1639	1.1601
D4	1.1813	1.1772

As seen from Figure 1, there are two different types of dianhydrides both being very extended in size. The dianhydrides A and B [19,20] have a very bulky structure while the dianhydrides C and D [22,23] are rather flat as the geometry optimisations show (Figure 3). The geometry optimisations also show that in between the dianhydride couples (A/B and C/D) exchanging the $Si(Me)_3$-group with the $C(Me)_3$-group does not significantly change the geometry of the respective dianhydride. Except for the diamine 1 [21] being very bulky as well and structurally comparable to some diamines Langsam et al. examined [1], Kim and coworkers used the common diamines 6FDA (2), MDA (3) and ODA (4). The experimentally measured oxygen permeabilities (P) vary for the polyimides A and B from high values of around 121 (A-1), 110 (B-2) and 105 (A-2) Barrer to smaller ones of 43 (B-3) and 31 (B-4) Barrer, while the polyimides C and D have permeabilities from 56 (C-2) Barrer down to 14 (C-4) and 13 (D-4) Barrer.

It should be noticed that looking at the permeabilities pairwise, i.e. the Si-containing structures and their C-containing counterparts, the P-values for the Si-containing polyimides are consistently higher than for the C-containing ones, except for A-2:B-2, where the C-containing structure is higher in permeability than the Si-containing one. The respective P-differences are, however, not very large

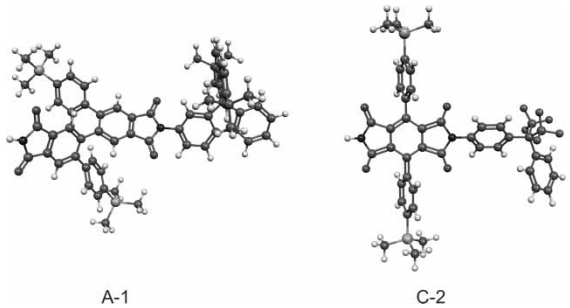

Figure 3. Optimised geometrical structures of A-1 and C-2. While A-1 has a very bulky structure, C-2, especially looking at the dianhydride, is quite flat.

and considering that the error of the experimental measurements is around 10% of the *P*-value, the data pairs A-2:B-2, C-2:D-2 and C-4:D-4 could be considered equal in their permeation values. The considerably higher difference in permeability for the A-1:B-1 pair is a bit unexpected. While all the other pairs differ by not more than 21 Barrer from each other usually a lot less), the difference of the *P*-values for this pair is 69 Barrer. Since, in the following discussion, A-1 and B-1 are also the only polymers that fall far out of the recognisable correlation between atomic structure and macroscopic transport parameters, it is assumed that either A-1 or B-1 might be influenced by some systematic error in the measured permeability.

The calculated size distributions of the free volume regions accessible for an oxygen molecule are given for all investigated polyimides in Figure 4, for groups A and B and in Figure 5 and for the groups C and D. Looking at the free volume analysis, the graphs follow the same trend, as the permeabilities, the Si-containing polyimides have a larger accessible free volume than their carbon counterparts, see also Table 5. Looking at these data the FAV behaviour follows:

$$\text{FAV-A-2} > \text{FAV-A-3} > \text{FAV-A-4} > \text{FAV-A-1},$$

$$\text{FAV-B-2} > \text{FAV-B-1} > \text{FAV-B-3} = \text{FAV-B-4},$$

$$\text{FAV-C-2} > \text{FAV-C-3} > \text{FAV-C-4},$$

$$\text{FAV-D-2} > \text{FAV-D-3} > \text{FAV-D-4},$$

while the permeabilities are

$$\text{PA-1} > \text{PA-2} > \text{PA-3} > \text{PA-4},$$

$$\text{PB-2} > \text{PB-1} > \text{PB-3} > \text{PB-4},$$

$$\text{PC-2} > \text{PC-3} > \text{PC-4},$$

$$\text{PD-2} > \text{PD-3} > \text{PD-4}.$$

The groups B, C and D show the same order in the sequences of the FAV and the *P*-values. An exception are B-3 and B-4 showing the same value of FAV, but having different permeabilities (43 and 31 Barrer, respectively). Group A shows an inconsistency regarding the polyimide A-1. The FAV and the *P*-value do not match in the way that A-1 shows the smallest FAV value in its group, but has the highest permeability. Since in the following discussion A-1 is also the only polymer extremely falling out of the recognisable correlation between atomic structure and macroscopic transport parameters, it is assumed that B-1 might be influenced by some systematic error in the measured permeability.

All polyimides show a maximum distribution for cavities with a radius of $2\text{–}4 \times 10^{-10}$ m). Additionally, some of the polyimides have a second maximum for cavities >5 which might be important for the permeability as stated in the literature [30,31]. Table 6 shows the percentages of the FAV-elements with radii $>5 \times 10^{-10}$ m. It can be seen that the Si-containing structures have a higher percentage of cavities $>5 \times 10^{-10}$ m than their counterparts containing C. In-between the groups B, C and D, the decrease of the percentage of FAV goes along with the decrease

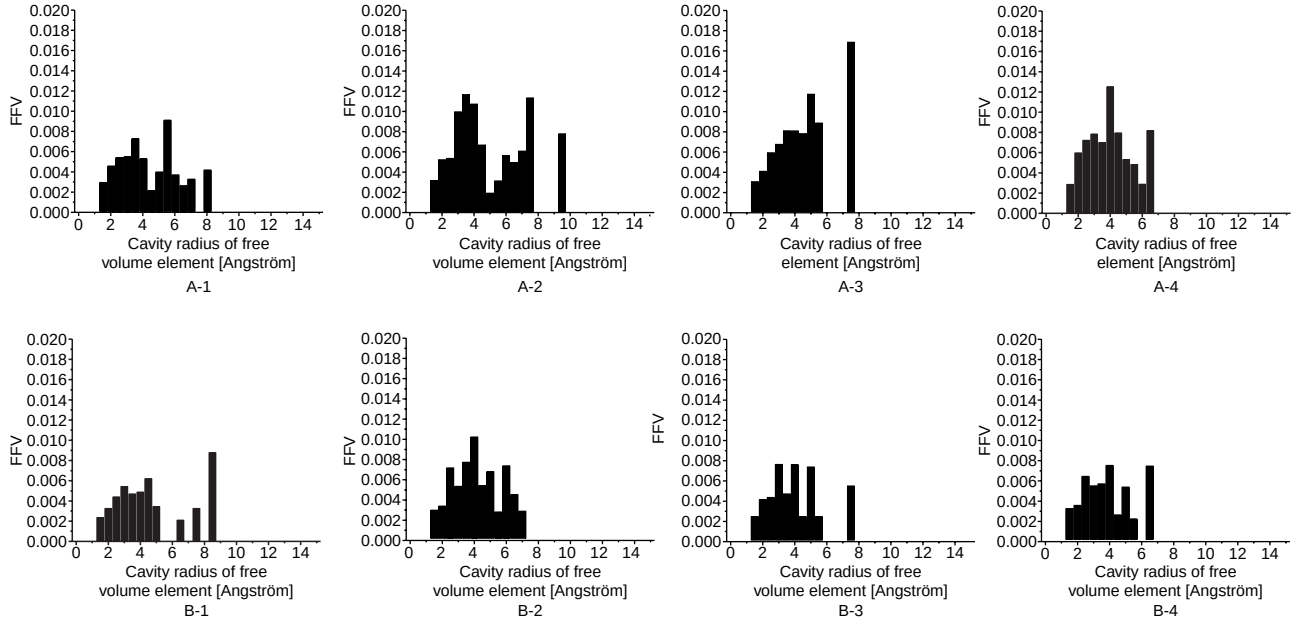

Figure 4. Bar-graph size distribution of free volume elements accessible for O_2 for the groups A and B.

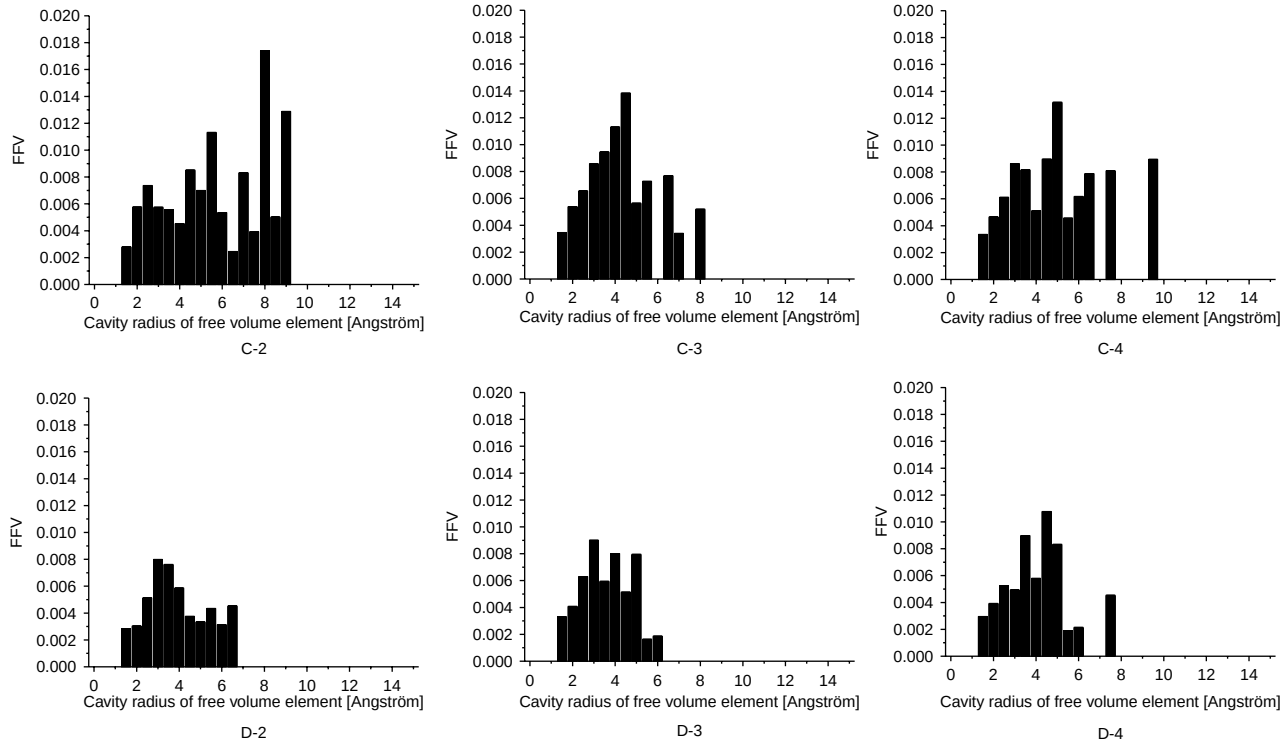

Figure 5. Bar-graph size distribution of free volume elements accessible for O_2 for the groups C and D.

in permeability. Group A is again the exception, where A-1 is second highest and A-2 shows the highest value.

Summarising the main result from the FAV analysis, polyimides containing Si have a higher free volume and cavities of bigger radii than their C-containing counterparts. Another parameter to discuss is the MSD, describing the self-diffusion of the polymer chain segments. It is defined as

$$\mathrm{MSD}(t) = \langle \Delta r_i(t)^2 \rangle = \langle (r_i(t) - r_i(o))^2 \rangle \qquad (1)$$

with $r_i(t) - r_0(t)$ being the distance travelled by molecule i over the time t. The MSD is an average over all time intervals and molecules.

Figures 6 and 7 show the MSD for the whole molecule for the groups A, B and C, D, respectively.

The MSD results for the whole molecules reveal that the Si-containing structures show always higher self-diffusion than the respective C-containing ones. Figures 8–10 contain respective results for the backbone and side-group mobilities.

Table 5. Calculated accessible free volumes (FAV) for oxygen, a positron and a particle $r = 0.4 \times 10^{-10}$ m and the estimated free volume (FFV).

Polyimide	FAV (O_2)	FAV (Positron)	FAV (0.4)	Estimated FFV (0.0)	P (O_2) ($7{,}5005 \times 10^{-18}$ m^2/s Pa)
A-1	0.058	0.211	0.310	0.330	121
A-2	0.092	0.275	0.330	0.350	105
A-3	0.080	0.196	0.328	0.405	61
A-4	0.072	0.232	0.324	0.360	52
B-1	0.049	0.261	0.298	0.305	52
B-2	0.064	0.173	0.313	0.390	110
B-3	0.047	0.191	0.306	0.340	43
B-4	0.047	0.202	0.310	0.340	31
C-2	0.114	0.302	0.341	0.345	56
C-3	0.094	0.275	0.338	0.340	32
C-4	0.088	0.264	0.334	0.340	14
D-2	0.071	0.234	0.349	0.380	50
D-3	0.053	0.225	0.319	0.330	20
D-4	0.059	0.226	0.316	0.330	13

Table 6. FAV for oxygen. Shown are as well the fraction of cavities smaller than 5 and bigger than 5 and the percentage of the cavities greater than 5 of the all over FAV.

Polyimide	P (O_2) (7,5005 $\times 10^{-18}$ m^2/s Pa)	FAV (O_2)	$<5\times10^{-10}$ m	$>5\times10^{-10}$ m	Percentage of FAV $>5\times10^{-10}$ m
A-1	121	0.058	0.036	0.022	0.381
A-2	105	0.092	0.054	0.038	0.415
A-3	61	0.080	0.055	0.025	0.313
A-4	52	0.072	0.056	0.016	0.222
B-1	52	0.049	0.035	0.014	0.286
B-2	110	0.064	0.047	0.017	0.265
B-3	43	0.047	0.039	0.008	0.170
B-4	31	0.047	0.040	0.007	0.148
C-2	56	0.114	0.047	0.067	0.585
C-3	32	0.094	0.058	0.036	0.380
C-4	14	0.088	0.064	0.023	0.268
D-2	50	0.071	0.039	0.012	0.169
D-3	20	0.053	0.050	0.003	0.066
D-4	13	0.059	0.051	0.002	0.033

Compared to the side-groups the backbones are very stiff, but in this connection the C-containing polyimides are more flexible than their Si-counterparts. This is in good agreement with the energetic potential for the dihedral rotation around the central C—C-bond Figure 11 of A and B, as it was obtained from a systematic conformational search procedure applying the Discover module of the MS Modeling software of Accelrys. While for the case of B the rotational barrier reaches not more than 100 kJ/mol, the barrier for A is extremely high.

For the side-groups the opposite effect is observed, i.e. the Si-containing ones are more flexible. The suggestion lies close, taking the results of the free volume also into account, that the size of the Si atom is the most important cause of the observed differences in free volume distribution and flexibility of the side-groups. As the Si

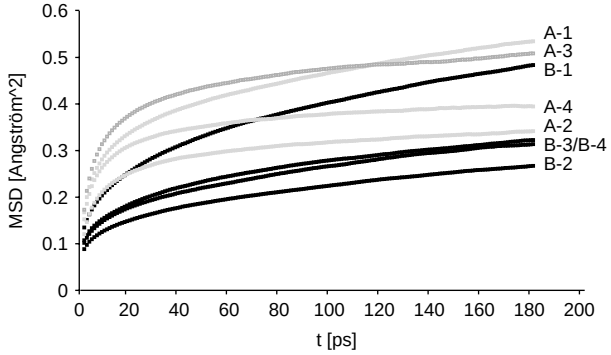

Figure 6. MSD versus the time for the groups A and B.

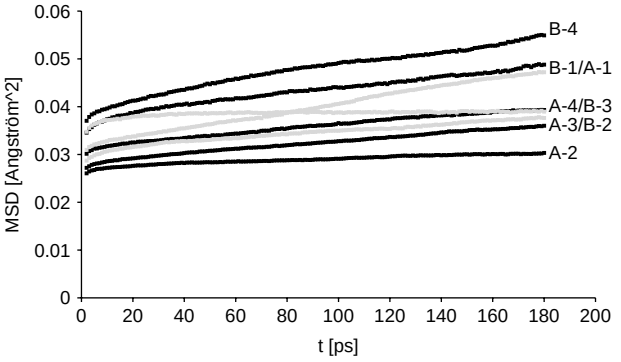

Figure 8. MSD of the backbone versus the time for the groups A and B.

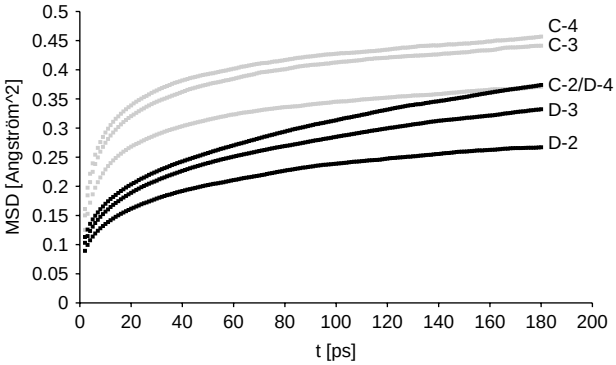

Figure 7. MSD versus the time for the groups C and D.

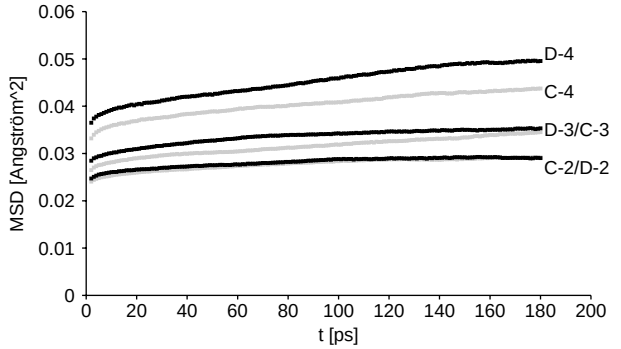

Figure 9. MSD of the backbone versus the time for the groups C and D.

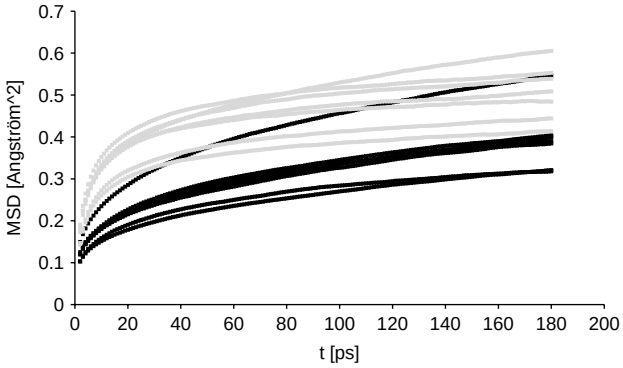

Figure 10. MSD of the sidechain versus the time for all groups. The grey lines represent the Si-containing molecules, the black lines the C-containing ones.

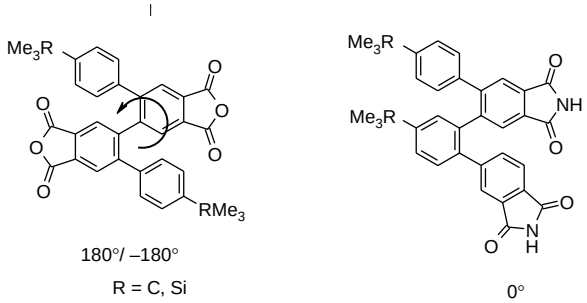

Figure 11. Dianhydride structure showing the conformation at 0° and 180/− 180°, respectively.

is a lot bigger than the carbon, it needs more space and the packing is therefore looser. As the packing is looser, there is more free volume and the sidechains are able to move more. On the other hand, the backbone for the dianhydride A due to the attached bulky Si(Me_3) side-groups is less flexible concerning the rotation around the central C—C-bond. The backbone flexibilities of the related pairs of groups C and D (e.g. C2:D2; C3:D3; C4:D4) are closer to each other especially for C-3:D-3 and C-2:D-2. Owing to the very stiff structure of the involved dianhydrides the main mobility contribution belongs to the respective diamines, being the same for each pair, which is why their MSD curves lie close together. The size of the Si does not influence the flexibility as much as in the cases of A and B, because the PMDA structure in the centre of the dianhydride is not flexible at all, so that the two Si-containing sidechains of each repeat unit do not interfere with each other as much as in the case of A and B.

Taking a closer look at Figure 10, the grey and the black lines crossing each other at 280 ps on top of the diagram present the polyimides A-1 and B-1. At the beginning the flexibility is quite low of the sidechains of B-1, but after time it is as flexible as A-1. While all the other structures are pretty parallel to each other in the MSD diagram, A-1 and B-1 cross. A MSD run over 5 ns, Figure 12 shows that after crossing the two curves run

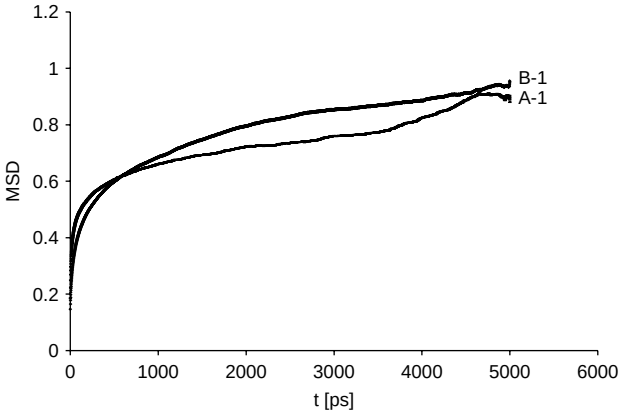

Figure 12. MSD versus the time for A-1 and B-1.

as well parallel to each other. This supports again the earlier mentioned idea that the experimentally obtained *P*-value for A-1 might be too high and that it should be closer to the one of B-1 as in all the other cases.

4. Conclusions

Parallel to the finding that the oxygen permeabilities between Si-containing polyimides and their C-containing counterparts typically are higher for the Si-case, these polymers also differ in their behaviour concerning the free volume and the MSD the way that the Si-containing structure have a higher free volume and are more flexible in their side-groups. This is due to the fact that the Si atom is bigger than a C atom and that because of that it needs more space. The more space there is the more the sidechains can move and the more free volume there is. The backbone of the Si-containing polyimides, however, is less flexible than the carbon ones especially in the case of the groups A and B as the big Si(Me_3) group makes a rotation around the centred C—C bond energetically more demanding.

Acknowledgements

The authors like to thank the European Commission 6th Framework Program Project MULTIMATDESIGN 'Computer aided molecular design of multifunctional materials with controlled permeability properties' for financial support.

References

[1] M. Langsam, *Polyimides for gas separation*, Chapter 22, in *Fundamentals and Applications*, K.J. Mittal, ed., Marcel Dekker, New York, 1996.

[2] M. Langsam and W.F. Burgoyne, *Effects of diamine monomer structure on the gas permeability of polyimdes. I. Bridged diamines*, J. Polym. Sci. Part A Polym. Chem. 31 (1993), pp. 909–921.

[3] S.A. Stern, Y. Mi, H. Yamamoto, and A.K. St. Clair, *Structure/permeability relationships of polyimide membranes. Applications to the separation of gas mixtures*, J. Polym. Sci. Part B Polym. Phys. 27 (1989), pp. 1887–1909.

[4] K. Tanaka, H. Kita, K. Okamoto, A. Nakamura, and Y. Kusuki, *Gas permeability and permselectivity in polyimides based on 3,3′,4,4′-biphenyltetracarboxylic dianhydride*, J. Membr. Sci. 47 (1989), pp. 203–215.

[5] M.R. Coleman and W.J. Koros, *Isomeric polyimides based on fluorinated dianhydrides and diamines for gas separation applications*, J. Membr. Sci. 50 (1990), pp. 285–297.

[6] K. Tanaka, H. Kita, M. Okano, and K. Okamoto, *Permeability and permselectivity of gases in fluorinated and non-fluorinated polyimides*, Polymer 33 (1992), pp. 585–592.

[7] K. Tanaka, M. Okano, H. Toshino, H. Kita, and K. Okamoto, *Effect of methyl substituents on permeability and permselectivity of gases in polyimides prepared from methyl-substituted phenylenediamines*, J. Polym. Sci. Part B Polym. Phys. 30 (1992), pp. 907–914.

[8] S.A. Stern, Y. Liu, and W.A. Feld, *Structure/permeability relationships of polyimides with branched or extended diamine moieties*, J. Polym. Sci. Part B Polym. Phys. 31 (1993), pp. 939–947.

[9] K. Matsumoto, P. Xu, and T. Nishikimi, *Gas permeation of aromatic polyimides. II. Influence of chemical structure*, J. Membr. Sci. 81 (1993), pp. 23–30.

[10] K.C. O'Brien, W.J. Koros, and G.R. Husk, *Polyimide materials based on pyromellitic dianhydride for the separation of carbon dioxide and methane gas mixtures*, J. Membr. Sci. 35 (1988), pp. 217–230.

[11] T.H. Kim, W.J. Koros, G.R. Husk, and K.C. O'Brien, *Relationship between gas separation properties and chemical structure in a series of aromatic polyimides*, J. Membr. Sci. 37 (1988), pp. 45–62.

[12] S.L. Liu, M.L. Chng, T.S. Chung, K. Goto, S. Tamai, K.P. Pramoda, and Y.J. Tong, *Gas-transport properties of indan-containing polyimides*, J. Polym. Sci. B 42 (2004), pp. 2769–2779.

[13] C. Staudt-Bickel and W.J. Koros, *Improvement of CO_2/CH_4 separation characteristics of polyimides by chemical crosslinking*, J. Membr. Sci. 155 (1999), pp. 145–154.

[14] S.L. Liu, R. Wang, T.S. Chung, M.L. Chng, Y. Liu, and R.H. Vora, *Effect of diamine composition on the gas transport properties in 6FDA-durene/3,3′-diaminodiphenyl sulfone copolyimides*, J. Membr. Sci. 202 (2002), pp. 165–176.

[15] S.L. Liu, R. Wang, Y. Liu, M.L. Chng, and T.S. Chung, *The physical and gas permeation properties of 6FDA-durene/2,6-diaminotoluene copolyimides*, Polymer 42 (2001), pp. 8847–8855.

[16] A. Shimazu, T. Miyazaki, T. Matsushita, M. Maeda, and K. Ikeda, *Relationships between chemical structures and solubility, diffusivity, and permselectivity of 1,3-butadiene and* n*-butane in 6FDA-based polyimides*, J. Polm. Sci. B 37 (1999), pp. 2941–2949.

[17] A. Shimazu, T. Miyazaki, M. Maeda, and K. Ikeda, *Relationships between the chemical structures and the solubility, diffusivity, and permselectivity of propylene and propane in 6FDA-based polyimides*, J. Polym. Sci. B 38 (2000), pp. 2525–2536.

[18] W.H. Lin, R.H. Vora, and T.S. Chung, *Gas transport properties of 6FDA-durene/1,4-phenylenediamine (pPDA) copolyimides*, J. Polym. Sci. B Polym. Phys. 38 (2000), pp. 2703–2713.

[19] Y.-H. Kim, H.-S. Kim, S.-K. Ahn, S.O. Jung, and S.-K. Kwon, *Synthesis of new highly organosoluble polyimides bearing a noncoplanar twisted biphenyl unit containing* t*-butyl phenyl group*, Bull. Korean Chem. Soc. 23 (2002), pp. 933–934.

[20] H.-S. Kim, Y.-H. Kim, S.-K. Ahn, and S.-K. Kwon, *Synthesis and characterization of highly soluble and oxygen permeable new polyimides bearing a noncoplanar twisted biphenyl unit containing* tert*-butylphenyl or trimethylsilyl phenyl groups*, Macromolecules 36 (2003), pp. 2327–2396.

[21] Y.-H. Kim, H.-S. Kim, and S.-K. Kwon, *Synthesis and characterisation of highly soluble and oxygen permeable new polyimides based on twisted biphenyl dianhydride and spirofluorene diamine*, Macromolecules 38 (2005), pp. 7950–7956.

[22] Y.H. Kim, S.-K. Ahn, H. Sun Kim, and S.-K. Kwon, *Synthesis and characterization of new organosoluble and gas-permeable polyimides from bulky substituted pyromellitic dianhydrides*, J. Polym. Sci. A: Polym. Chem. 40 (2002), pp. 4288–4296.

[23] Y.-H. Kim, S.-K. Ahn, and S.-K. Kwon, *Synthesis and characterization of novel polyimides containing bulky trimethylsilylphenyl group*, Bull. Korean Chem. Soc. 22 (2001), p. 451.

[24] H. Sun and D. Rigby, *Polysiloxanes:* ab initio *force field and structural, conformational and thermophysical properties*, Spectrochim Acta A 53 (1997), pp. 1301–1323.

[25] D. Rigby, H. Sun, and B.E. Eichinger, *Computer simulations of poly(ethylene oxide): Force field, pvt diagram and cyclization behaviour*, Polym. Int. 44 (1997), pp. 311–330.

[26] D. Hofmann, L. Fritz, J. Ulbrich, C. Schepers, and M. Böhning, *Detailed atomistic molecular modeling of small molecule diffusion and solution processes in polymeric membrane materials*, Macromol. Theor. Simul. 9 (2000), pp. 293–327.

[27] D. Hofmann, M. Entrialgo-Castaño, A. Lerbret, M. Heuchel, and Y. Yampolskii, *Molecular modeling investigations of free volume distributiona in stiff chain polymers with conventional and ultrahigh free volume: Comparison between molecular modeling and positron lifetime studies*, Macromolecules 36 (2000), pp. 8528–8538.

[28] Y. Xiao, T.-S. Chung, M.L. Chng, S. Tamai, and A. Yamaguchi, *Structure and properties relationships for aromatic polyimides and their derived carbon membranes: Experimental and simulation approaches*, J. Phys. Chem. B 109 (2005), pp. 18741–18748.

[29] J. Bicerano, *Prediction of Polymer Properties*, Marcel Dekker, Inc., New York, 1993.

[30] M. Heuchel, D. Hofmann, and P. Pullumbi, *Molecular modeling of small-molecules permeation in polyimides and its correlation of free-volume distributions*, Macromolecules 37 (2004), pp. 201–214.

[31] B.R. Wilks, W.J. Chung, P.J. Ludovice, M.R. Rezac, P. Meakin, and A. Hill, *Impact of average free-volume element size on transport in stereoisomers of polynorborne. I. Properties at 35°C*, J. Polym. Sci. B Polym. Phys. 41 (2003), pp. 2185–2199.